Journal of Alloys and Compounds 507 (2010) 425–428

Contents lists available at ScienceDirect

Journal of Alloys and Compounds

journal homepage: www.elsevier.com/locate/jallcom

Large quadratic electro-optic properties of ferroelectric base $0.92Pb(Mg_{1/3}Nb_{2/3})O_3$–$0.08PbTiO_3$ single crystal

Yanting Lin[a,b,*], Bo Ren[a,b], Xiangyong Zhao[b], Dan Zhou[a,b], Jing Chen[a,b], Xiaobing Li[a,b], Haiqing Xu[a], Di Lin[a], Haosu Luo[a]

[a] The State Key Laboratory of High Performance Ceramics and Superfine Microstructure, Shanghai Institute of Ceramics, Chinese Academy of Sciences, 215 Chengbei Road, Jiading, Shanghai 201800, China
[b] Graduate School of the Chinese Academy of Sciences, Beijing 10039, China

ARTICLE INFO

Article history:
Received 6 April 2009
Accepted 12 June 2010
Available online 23 June 2010

PACS:
78.20.Ci
46.40.Cd
42.25.Lc

Keywords:
PMN–0.08PT single crystal
Refractive indices
Transmission spectrum
Quadratic electro-optic coefficient

ABSTRACT

Large Kerr effect in $0.92Pb(Mg_{1/3}Nb_{2/3})O_3$–$0.08PbTiO_3$ (PMN–0.08PT) single crystal has been observed. The effective quadric electro-optical coefficient $(R_{11} - R_{12})$ of PMN–0.08PT single crystal is measured by a Senarmont compensator method. The refractive indices and extinction coefficient of PMN–0.08PT single crystal ranging from 300 to 1700 nm have been measured by variable angle spectroscopic ellipsometry (VASE). The transmission character of PMN–0.08PT single crystal in the range of 300–2200 nm has been investigated by UV–visible–NIR spectrometer. The transmission ratio is 65% in the range of 600–2100 nm and the calculated reflection loss is about 20%. The effective quadric electro-optical coefficient $(R_{11} - R_{12})$ is calculated to be $8.19 \times 10^{-16}\ m^2\ V^{-2}$ and the $n^3(R_{11} - R_{12})$ is $141.8 \times 10^{-16}\ m^2\ V^{-2}$ at 514.5 nm, respectively. The V_π of the sample is 632 V.

1. Introduction

Optical materials with large electro-optic (EO) coefficients are highly desirable for uses in optical communications, optical signal processing, and other commercial applications. In many EO applications, the modulation of light is usually based on the Pockels effect (first-order EO effect) or on the Kerr effect (second-order EO effect). The relaxor ferroelectric crystals $(1-x)$PMN–xPT are very well known for its high electromechanical coupling factor, piezoelectric coefficients and field induced strain response [1,2]. Large linear EO coefficients in $(1-x)$PMN–xPT ($x = 0.24$–0.40) single crystals near the morphotropic phase boundary (MPB) have been reported in recent years [3,4]. Remarkable quadratic electro-optic coefficient of PMN–xPT ($0.15 \le x \le 0.4$) thin films also have been found by Lu et al. [5]. These optical properties have been attributed to a phase transition between the tetragonal and the rhombohedral phases due to the electric field, which is associated with large changes in the crystal lattice constants and the refractive index [6–9]. However, the quadric EO coefficients of cubic phase $(1-x)$PMN–xPT ($x < 0.1$) single crystals have not been reported. For there is a phase transition between the cubic and the rhombohedral phases in $(1-x)$PMN–xPT ($x < 0.1$) single crystals near room temperature, electric-field may induce large change in refractive index of the cubic $(1-x)$PMN–xPT ($x < 0.1$) single crystals. In this letter, the Kerr effect of PMN–0.08PT single crystal was investigated by a modified Senarmont compensator method. The effective quadric electro-optical coefficient and half-wave voltage are calculated. The refractive indices and transmission character of the single crystal were studied and the reflection loss was also discussed.

2. Experimental procedure

Large size and high quality PMN–0.08PT single crystal was grown by modified Bridgman method [10,11]. The single crystal was oriented using X-ray diffractometer. For VASE measurement, the sample was cut along ⟨0 0 1⟩ direction. The surface for light reflection was optically polished. The VASE measurement was carried out in the wavelength range of 300–1700 nm with 5 nm steps at incidence angle of 65° by a W-VASE32 TM Ellipsometer with synchronously rotating polarizer and analyzer at room temperature. For transmission measurement, the incident light was perpendicular to the (0 0 1) faces. Transmission spectrum was measured by a JASCO's V-570 UV–visible–NIR spectrometer in the wavelength range from 300 to 2200 nm at room temperature. EO measurement was performed by a modified Senarmont setup as shown in Fig. 1. The sample was cut into cube with 3 mm × 3 mm × 6 mm. The E

* Corresponding author at: Shanghai Institute of Ceramics, Chinese Academy of Sciences, 215 Chengbei Road, Jiading, Shanghai, China.
Tel.: +86 21 6998 7759; fax: +86 21 5992 7184.
E-mail address: linyanting@gmail.com (Y. Lin).

0925-8388/$ – see front matter © 2010 Elsevier B.V. All rights reserved.
doi:10.1016/j.jallcom.2010.06.068

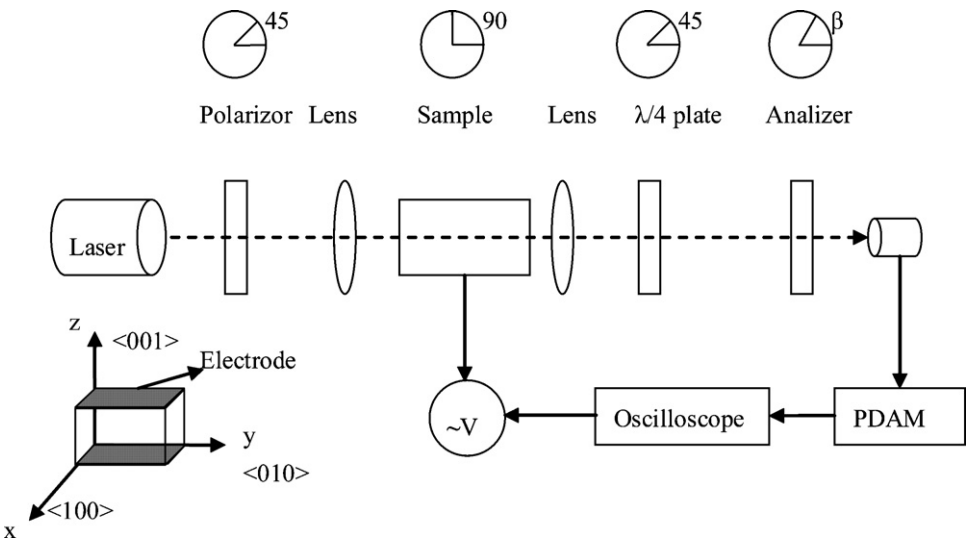

Fig. 1. Experiment arrangement of the optical and electronic components in the modified Senarmont system.

field was applied across the ⟨0 0 1⟩ direction (3 mm thickness) and the incident light propagated along the ⟨1 0 0⟩ direction (6 mm thickness). The polarization direction of polarizer was set at 45° to the principal c axis of the crystal. Thus the quadric EO coefficient is defined by, $(R_{11} - R_{12}) = \Delta n/(1/2)n^3E^2$, where Δn is the induced birefringence, n is the refractive index of the undistorted indicatrix $(R_{11} - R_{12})$ is the effective quadratic electro-optic coefficient, and E is the applied field.

3. Results and discussion

3.1. Refractive indices and dispersion equation

The refractive indices at different wavelength of PMN–0.08PT single crystal were investigated by the spectroscopic ellipsometry. The theory for ellipsometric analysis is based on the Fresnel reflection or transmission equations for polarized light encountering boundaries in planar multi-layered materials. These come from solutions to Maxwell's equations. The ellipsometry measurements are normally expressed in terms of Psi (Ψ) and Delta (Δ):

$$\rho = \tan(\Psi) \cdot e^{i\Delta} = \frac{r_p}{r_s} \tag{1}$$

where r_p and r_s are the complex Fresnel reflection coefficients for p^- (in the plane of incidence) and s^- (perpendicular to the plane of incidence) polarized light, respectively. Spectroscopic ellipsometry (SE) measures the complex ratio as a function of wavelength. For bulk isotropic sample investigated here, its complex refractive index ($\tilde{n} = n + ik$) can be revealed automatically by comparing the computer modeling data with the experimental data [10–12]. Fig. 2 shows the wavelength dependence of the refractive indices and extinction coefficients at room temperature for PMN–0.08PT single crystal, respectively. The result shows that PMN–0.08PT single crystal has lager refractive indices at different wavelength and the refractive indices and extinction coefficients strongly depend on the wavelength especially in the UV region. This is similar to other ABO_3-type perovskite structure compounds [13,14]. The extinction coefficients decrease and become small when the wavelength is above 500 nm. This indicates that PMN–0.08PT single crystal is transparent in the visible light region. Because of the similar BO_6 octahedron unit structure, they have analogous energy band structure determining the refractive indices [13,14].

From the well known simple dispersion theory, the refractive index can be given by typical Sellmeier dispersion equation:

$$n^2 = A + \frac{B}{\lambda^2 - C} - D\lambda^2 \tag{2}$$

where A, B, C and D are all constants and λ is wavelength in microns. These constants can be obtained by the least squares fitting of the equation with the refractive indices measured by VASE. Thus the Sellmeier dispersion equation of n for PMN–0.08PT is

$$n^2 = 5.8255 + \frac{0.191154}{\lambda^2 - 0.042151} + 0.022096\lambda^2 \tag{3}$$

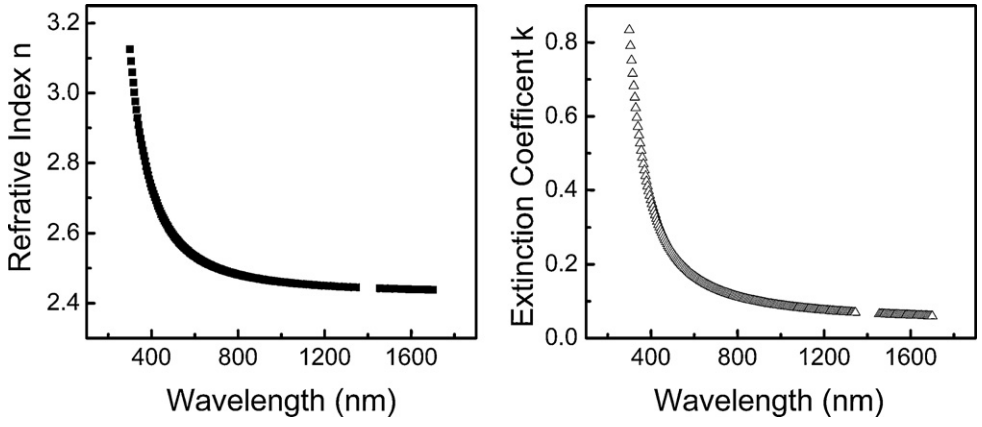

Fig. 2. The refractive indices and extinction coefficients of PMN–0.08PT single crystal measured at different wavelengths.

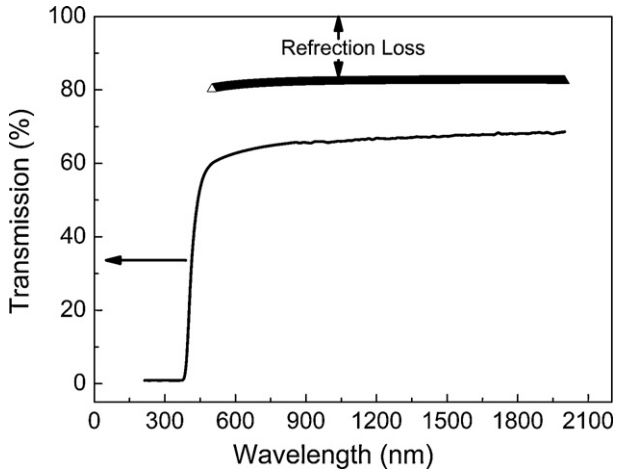

Fig. 3. Transmission ratio and reflection loss of PMN–0.08PT single crystal.

By the dispersion equation, the refractive indices of PMN–0.08PT single crystal can be calculated. For example, at the wavelength of 514.5 nm, $n = 2.5869$.

3.2. Transmission spectrum

The transmission spectrum of the sample with 2.40 mm thickness is shown in Fig. 3. The crystal is transparent in visible region; the curves roll off in near 450 nm. The transmittance begins to increase abruptly at around 400 nm, indicating an optical absorption edge in ultraviolet region, and continues into the IR region without any obvious change. In the range of 500–2100 nm the transmission ratio of PMN–0.08PT single crystal is about 65%. This is similar to what was observed for most crystals with oxygen-octahedral perovskite structure [3,4].

From the transmission characterization, it shows that the optical absorption is very small at higher wavelength range. In general, optical transmission relates to reflection losses and scattering losses. The reflection loss of the light at two surfaces was calculated using the refractive indices and by the Fresnel expression $R = (n-1)^2/(n+1)^2$ and was also shown in Fig. 3. For PMN–0.08PT single crystal has large refractive indices, the reflection loss is near 20%. It is well known that $(1-x)$PMN–xPT ($x < 0.1$) single crystals are far away from the MPB phase. Thus high optical qualities and visible domains-walls free $(1-x)$PMN–xPT ($x < 0.1$) single crystals may easier to obtained than $(1-x)$PMN–xPT ($x = 0.24$–0.40) single crystals near MPB phase.

3.3. Quadratic electro-optic coefficient

At room temperature, the PMN–0.08PT single crystal has pseudo cubic structure [15]. When the polarization direction of the incident light is set at 45° to the natural birefringence axes of the sample, the effective change for the refractive index in the Senarmont system is

$$\Delta n = \frac{1}{2} n^3 (R_{11} - R_{12}) E^2 \tag{4}$$

where Δn is the induced birefringence, n is the refractive index of the undistorted indicatrix, $(R_{11} - R_{12})$ is the effective quadratic electro-optic coefficient, and E is the applied field.

A dynamic (ac) method was employed to measure the effective Quadric EO coefficients for it is more precise and sensitive than the static (dc) method [18]. In the Senarmont system described above, the equation of the transfer function of the light intensity

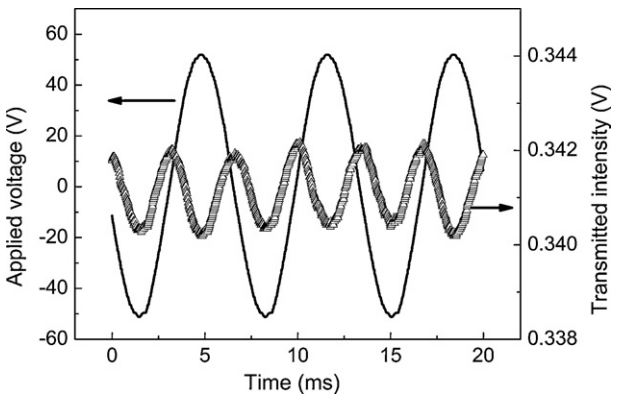

Fig. 4. Modulated transmitted intensity curve as function of applied voltage V.

transmitted through the setup can be written as [16]:

$$T = \left(\frac{I}{I_0}\right) = T_0 \sin^2\left[\left(\frac{\Gamma}{2}\right) - \beta\right] \tag{5}$$

where I_0 is the incident light intensity, I is the output light intensity and T_0 is the transmission factor expressing the losses of light throughout the system. When the condition $\Gamma_m < 0.1$ rad is satisfied, with a treatment of the transmission Eq. (5) by means of Bessel functions, the amplitude of the modulated intensity signal at the maximum linearity point is equal to [17]

$$I_m = I_\omega \approx \left(\frac{T_0 I_0}{2}\right) \Gamma_m \tag{6}$$

In practice, the optical signal is converted to a voltage change through

$$v = S_0 I_m \text{ and } v_{p-p} = S_0 T_0 I_0 \tag{7}$$

where S_0 is the constant of photo-response of the photodetection system. If the transmission factor T_0 is completely compensated, the phase retardation Γ_m induced by the applied field can be determined from Eqs. (6) and (7) by

$$\Gamma_m = \frac{2v}{v_{p-p}} \tag{8}$$

Thus the effective EO coefficient can be calculated from

$$(R_{11} - R_{12}) = \frac{\lambda d^2 \Gamma_m}{\pi n^3 L {V_m}^2} \tag{9}$$

where λ is the incident light wavelength, d is the electrode spacing, L is the length along the light path, n is the reflective index at the incident light, and V_m is the maximum value of the applied ac field. The transmitted intensity dependence on applied voltage of PMN–0.08PT single crystal is shown in Fig. 4. Thus $(R_{11} - R_{12})$ and $n^3(R_{11} - R_{12})$ are calculated to be $8.19 \times 10^{-16}\ \mathrm{m^2\,V^{-2}}$ and $141.8 \times 10^{-16}\ \mathrm{m^2\,V^{-2}}$ at 514.5 nm,respectively. Quadric EO coefficient of some optical materials is also listed in Table 1 [5,17–19]. We can see that PMN–0.08PT single crystal has a larger quadric EO coefficient. It is more than two times than that of PLZT ceramics, which already has been used in variable optical attentunator [18]. When $\Gamma_m = \pi$, V_m is defined as half-wave voltage (V_π) and it is calculated to be 632 V by Eq. (9). The reason for the large quadric EO coefficient of PMN–0.08PT single crystal is the T_C of the crystal is very close to the room temperature and ferroelectric usually have large quadratic EO effect at the temperature around T_C. It maybe the electric-field could easily induce a changing in the crystal lattice constants and the refractive index of the crystal near this temperature.

Table 1
Quadric EO coefficient of some materials.

Quadric EO materials	$n^3(R_{11}-R_{12})\times10^{-16}(m^2/V^2)$	$(R_{11}-R_{12})\times10^{-16}\ (m^2/V^2)$	$R_{effect}\times10^{-16}\ (m^2/V^2)$	n	Reference
$Pb(Mg_{1/3}Nb_{2/3})O_3$ (ceramics)	24.2[a]			2.56	[17]
$Pb_{1-x}La_x(Zr_yTi_{1-y})_{1-x/4}O_3$(ceramics)			2.8[b]		[18]
(Pb,La)(Zr,Ti)O_3(films)			1.0[c]		[19]
PMN–*x*PT (films)			1.32[c]		[5]
PMN–0.08PT (crystal)	141.8	8.19		2.87	This work

[a] $\lambda = 624$ nm.
[b] $\lambda = 1550$ nm.
[c] $\lambda = 632.8$ nm.

4. Conclusion

The refractive indices PMN–0.08PT single crystal has been measured by spectroscopic ellipsometry in wavelength range from 300 to 1700 nm. Like other oxygen-octahedra ferroelectrics, the refractive indices of PMN–0.08PT single crystal are large strongly depend on the wavelength. The transmission ratio of PMN–0.08PT single crystal in range of 600–2200 nm is near 70% and the calculated reflection loss is about 20%. PMN–0.08PT single crystal has a large effective quadric electro-optical coefficient ($R_{11}-R_{12}$) at the room temperature, which is near its T_C. High transparent and large EO coefficient make PMN–0.08PT single crystal to be a promising candidate in optical devices.

Acknowledgments

This work was financially supported by the Ministry of Science and Technology of China through 863 Program (Grant No. 2008AA03Z410) and 973 Program (Grant No. 2009CB623305), the Natural Science Foundation of China (Grant Nos. 60837003, 50777065, and 50602047), Shanghai Municipal Government (Grant No. 08JC1420500) and the Innovation Fund of Shanghai Institute of Ceramics (Grant No. O99ZC4140G).

References

[1] G. Xu, H. Luo, P. Wang, H. Xu, Z. Yin, Chin. Sci. Bull. 45 (2000) 491.
[2] S.E. Park, T.R. Shrout, J. Appl. Phys. 82 (1997) (1804).
[3] X. Wan, H. Xu, T. He, D. Lin, H. Luo, J. Appl. Phys. 93 (2003) 4766.
[4] C.J. He, F.F. Wang, D. Zhou, X.Y. Zhao, D. Lin, H.Q. Xu, T.H. He, H.S. Luo, J. Phys. D: Appl. Phys. 39 (2006) 4337.
[5] Y.L. Lu, B. Gaynor, C. Hsu, G.H. Jin, M. Cronin-Golomb, F.L. Wang, J. Zhao, S.Q. Wang, P. Yip, A.J. Drehman, Appl. Phys. Lett. 74 (1999) 3038.
[6] Y. Lu, Z.Y. Cheng, S.E. Park, S.F. Liu, Q.M. Zhang, Jpn. J. Appl. Phys. 39 (2000) 141.
[7] Y. Barad, Y. Lu, Z.Y. Cheng, S.E. Park, Q.M. Zhang, Appl. Phys. Lett. 77 (2000) 1247.
[8] D.Y. Jeong, Y. Lu, V. Sharma, Q. Zhang, H.S. Luo, Jpn. J. Appl. Phys. 42 (2003) 4387.
[9] Y. Lu, Z.Y. Cheng, Y. Barad, Q.M. Zhang, J. Appl. Phys. 89 (2001) 5075.
[10] H. Luo, G. Xu, P. Wang, Z. Yin, Ferroelectrics 231 (1999) 97.
[11] H. Luo, G. Xu, H. Xu, P. Wang, Z. Yin, Jpn. J. Appl. Phys. 39 (2000) 5581.
[12] B. Johs, R.H. French, F.D. Kalk, W.A. McGahan, J.A. Woollam, Proc. SPIE 2253 (1994) 1098.
[13] M. Di Domenico Jr., S.H. Wemple, J. Appl. Phys. 40 (1969) 720.
[14] S.H. Wemple, M. DiDomenico Jr., J. Appl. Phys. 40 (1969) 735.
[15] V.A. Bokov, E. Mylnikova, Sov. Phys. Solid State 3 (1961) 613.
[16] M. Aillerie, N. Theïofanous, M.D. Fontana, Appl. Phys. B 70 (2000) 317.
[17] G.A. Smolenskii, N.N. Krainik, A.A. Berezhnoi, I.E. Mylnikova, Sov. Phys. Solid State 10 (1969) 2105.
[18] H. Jiang, Y.K. Zou, Q. Chen, Proc. SPIE 5644 (2005) 380.
[19] H. Adachi, T. Mitsuyu, O. Yamazaki, K. Wasa, J. Appl. Phys. 60 (1986) 736.